Received: 8 December 2021 | Revised: 17 January 2022 | Accepted: 20 January 2022

DOI: 10.1111/jnc.15582

Journal of Neurochemistry JNC The Official Journal of the International Society for Neurochemistry WILEY

ORIGINAL ARTICLE

Disruption of amphetamine sensitization by alteration of dendritic thin spines in the nucleus accumbens core

Wen Ting Cai[1] | Wha Young Kim[1] | Myung Ji Kwak[2] | Haeun Rim[2] | Seung Eun Lee[3] | Lars Björn Riecken[4] | Helen Morrison[4] | Jeong-Hoon Kim[1,2]

[1]Department of Physiology, Yonsei University College of Medicine, Seoul, Republic of Korea

[2]Department of Medical Sciences, Yonsei University College of Medicine, Seoul, Republic of Korea

[3]Virus Facility, Research Animal Source Center, Korea Institute of Science and Technology, Seoul, Republic of Korea

[4]Leibniz Institute on Aging, Fritz Lipmann Institute, Jena, Germany

Correspondence
Jeong-Hoon Kim, Department of Physiology, Yonsei University College of Medicine, Seoul, Republic of Korea.
Email: jkim1@yuhs.ac

Funding information
The National Research Foundation of Korea, Grant/Award Number: 2018R1A4A1025230, 2019R1A2C1011262 and 2019R1A2C2089518; National Research Foundation of Korea

Abstract

Repeated injections of psychomotor stimulants like amphetamine (AMPH) to rodents can induce behavioral sensitization, which represents a long-lasting craving that is usually observed in human addicts. Behavioral sensitization is characteristically maintained for a long duration, accompanied by structural plasticity in some brain areas involved in reward circuitry. For example, it increased dendritic spine densities in the nucleus accumbens (NAcc), which is considered to reflect neurophysiological changes at this site, leading to addictive behaviors. The ezrin, radixin, and moesin (ERM) proteins regulate spine maturity by modifying their phosphorylation at the C-terminal region. We previously showed that ERM phosphorylation is reduced by AMPH in the NAcc core, suggesting that ERM-mediated spine changes at this site might be associated with AMPH sensitization. To test this hypothesis, we administered AMPH to rats according to a sensitization development schedule, with lentivirus encoding a phosphomimetic pseudo-active mutant of radixin (Rdx T564D) in the NAcc core, and examined dendritic spines at this site. We found that compared to acute AMPH, AMPH sensitization increased thin spine density with a similar ratio of filopodia-like to mature thin spines. However, with Rdx T564D, the density of thin spines increased, with augmented filopodia-like thin spines, resulting in no AMPH sensitization. These results indicate that Rdx T564D forces thin spines to immaturity and thereby inhibits AMPH sensitization, for which an increase in mature thin spines is normally necessary. These findings provide significant clues to our understanding of the role of dendritic spines in mediating the development of psychomotor stimulant addiction.

KEYWORDS
amphetamine, locomotor sensitization, nucleus accumbens, radixin, dendritic spine

Abbreviations: AMPH, amphetamine; ANOVA, analysis of variance; ERM, ezrin, radixin, and moesin; GAPDH, glyceraldehyde 3-phosphate dehydrogenase; HEK293, human embryonic kidney 293; ICAM-5, intercellular cell adhesion molecule-5; IP, intra-peritoneal; GFP, green fluorescent protein; MSN, medium spiny neurons; NAcc, nucleus accumbens; PBS, phosphate buffered saline; PFA, paraformaldehyde; Rdx T564D, phosphomimetic pseudo-active mutant of radixin; RRID, Research Resource Identifier.

Wen Ting Cai and Wha Young Kim are co-first authors and contributed equally to this work.

1 | INTRODUCTION

Behavioral sensitization is manifested as enhanced increase in locomotor activity, when rodents are challenged with psychomotor stimulants such as amphetamine (AMPH) following pre-exposure of the same drugs (Anagnostaras, Schallert, & Robinson, 2002; Robinson & Berridge, 1993; Vezina, 2004). Once induced, behavioral sensitization is characteristically maintained for a long duration as a form of long-term memory contributing to the organism's incessant drug-seeking behaviors (Anagnostaras et al., 2002). As a result, this phenomenon has been widely established and employed as an animal model to investigate the escalating drug use and long-lasting craving in human addicts (Robinson & Berridge, 1993; Vezina, 2004).

Structural plasticity involving morphological changes of dendritic spines is generally considered to reflect the physiological and biochemical alterations in neuronal cells, which eventually contributes to behavioral changes (Brown et al., 2011; Chidambaram et al., 2019; Wang et al., 2013). For instance, it has been shown that stably maintained dendritic spines are associated with the formation and maintenance of long-term memories (Xu et al., 2009; Yang, Pan, & Gan, 2009). The nucleus accumbens (NAcc) is a neuronal substrate which mediates the rewarding and locomotor activating properties of addictive drugs. Interestingly, enhanced dendritic spine density in the NAcc has been reported in rats with sensitized behavioral patterns developed as a result of repeated exposure to psychomotor stimulants (Cahill et al., 2018; Christian et al., 2017; Li, Acerbo, & Robinson, 2004; Robinson & Kolb, 1997, 1999). However, it is not clear yet as to how the changes associated with dendritic spines contribute to persistent addictive behaviors.

The ezrin, radixin, and moesin (ERM) proteins share high degree of sequence homology among themselves and are generally known to contribute to determining the cell-shape and structural stability by bridging F-actin cytoskeleton to plasma membrane (Louvet-Vallée, 2000; Bretscher et al., 2002; Niggli & Rossy, 2008; Neisch & Fehon, 2011). In neuronal cells, they also play a critical role in regulating spine maturity. For example, when the ERM proteins are activated upon phosphorylation of their C-terminal threonine residue, they bind to cellular adhesion molecules like intercellular cell adhesion molecule-5 (ICAM-5), a specific protein found on dendrites of spiny neurons in the mammalian telencephalon, and assist them to maintain filopodia or spine immaturity (Furutani et al., 2007, 2012; Matus, 2005; Raemaekers et al., 2012; Yoshihara, De Roo, & Muller, 2009). However, whether ERM proteins are involved in the regulation of spine maturity in the NAcc, especially with respect to addictive behaviors, remains unidentified.

We have previously shown that ERM phosphorylation is curtailed by AMPH in the NAcc core (Kim, Jang, Shin, & Kim, 2013), suggesting that ERM-mediated spine changes at this site might be associated with AMPH sensitization. Thus, we aimed to examine whether AMPH-induced behavioral sensitization and accompanied dendritic spine changes are modulated, by oppositely regulating the phosphorylation levels of ERM against AMPH. For this purpose, we targeted radixin, which is the most abundant ERM proteins in the NAcc. We used a pre-designed lentivirus (Riecken et al., 2016), encoding radixin gene with a mutation at amino acid 564 residue at the C-terminal region, changing it from threonine (T) to aspartic acid (D). As a result, it functions as a phosphomimetic pseudo-active mutant (Rdx T564D) because of its structural resemblance to phosphorylated radixin, although it is not phosphorylated by itself (Furutani et al., 2007; Riecken et al., 2016).

2 | MATERIALS AND METHODS

2.1 | Subjects and drug

Male Sprague-Dawley rats (RRID: RGD 734476), 6 weeks olds weighing 200–230 g on arrival, were obtained from Orient Bio Inc. (Seongnam-si, Korea). The rats were housed three per cage, and had access to water and food ad libitum at all times. Colony rooms had a controlled room temperature (21°C) and a 12-h light/dark cycle (lights on at 8:00 am), and all experiments were conducted during the day. All animal use procedures were conducted according to an approved Institutional Animal Care and Use Committee protocol of Yonsei University College of Medicine (Ref. No. 2017-0194).

D-amphetamine sulfate (Cat. No. 1180004, United States Pharmacopeial) was dissolved in sterile 0.9% saline to a final working concentration of 1 mg/ml.

2.2 | Western blotting

Tissues were homogenized in lysis buffer (pH 7.4) containing 0.32 M sucrose, 2 mM EDTA, 1% SDS, 10 μg/ml aprotinin, 10 μg/ml leupeptin, 1mM phenylmethylsulfonyl fluoride, 10 mM sodium fluoride, and 1mM sodium orthovanadate. The concentration of protein was determined by using Pierce BCA Protein Assay Kit (Cat. No. 23227, Thermo Scientific Inc.). Samples were then boiled for 10 min and subjected to SDS-polyacrylamide gel electrophoresis. Proteins were separated and transferred electrophoretically to nitrocellulose membranes (Cat. No. 1620094, Bio-Rad), which were then blocked with 5 % bovine serum albumin (BSA) in PBS-T buffer [10 mM phosphate-buffered saline plus 0.05 % Tween-20]. Specific antibodies against phospho-ERM (specific to detect phosphorylated ezrin-radixin-moesin at threonine 567, 564 or 558, respectively; 1:500 dilution in PBS-T with 5% bovine serum albumin; Cat. No. 3141, Cell Signaling) and β-actin (1:10,000 dilution in PBS-T with 5% skim milk; RRID: AB 2223210, Abcam) were used to probe the blots. Primary antibodies were detected with peroxidase-conjugated secondary antibodies against rabbit IgG (1:2,000; Cat. No. K0211708, KOMA Biotech) or mouse IgG (1:5,000; RRID: AB 330924, Cell Signaling) diluted in PBS-T with 5% skim milk, followed by enhanced chemiluminescence reagents (Cat. No. LF-QC0101, Amersham Biosciences) and exposure to X-ray film. Band intensities were quantified based on densitometric values using Fujifilm Science Lab 97 Image Gauge software (version 2.54) (Fujifilm).

2.3 | Virus

The plasmids for lentiviral vectors containing copepod green fluorescent protein (copGFP) alone or copGFP with Rdx T564D were designed and kindly provided by Drs. Lars Björn Riecken and Helen Morrison at the Leibniz Institute on Aging, Fritz Lipmann Institute (Jena, Germany), and this material is available upon reasonable request. In brief, human radixin gene with a mutation at threonine 564 amino acid residue, resulting in its change to aspartic acid, and an additional FLAG-tag sequence (GACTACAAGGACGACGAC) at the N-terminal, was cloned in the lentiviral pCDH-CuO-MCS-EF1-copGFP vector (SparQ Dual Promoter [Cat. No. QM511B-1]; System Biosciences) (Riecken et al., 2016). Virus particles were generated using a third-generation lentiviral packaging systems at the Virus Facility, Research Animal Source Center, Korea Institute of Science and Technology (Seoul, Korea).

2.4 | Cell transfection and immunocytochemistry

Human embryonic kidney (HEK) 293 cell was purchased from the American Type Culture Collection (ATCC) (Cat. No. CRL-1573, ATCC). This cell line is not included as a commonly misidentified cell line by the International Cell Line Authentication Committee and has not been authenticated after acquisition. The cells were only used for experiments up to 15 passages. The cells were cultured in 1:1 mixture of Dulbecco's modified Eagle's medium (Cat. No. 10-013, Corning) and F-12 (Cat. No. 21127-022, Gibco), supplemented with 25 mM glucose, 4 mM L-glutamine, 1 mM sodium pyruvate, 10% heat-inactivated fetal bovine serum (Cat. No. 10082-147, Gibco), and 10000 units/ml penicillin-streptomycin (Cat. No. 15140-122, Gibco). The day before treatment of viruses, cells were transferred to coverslip (1×10^4 cells per coverslip) coated with 0.1 mg/ml Poly-D-Lysine (Cat. No. A-003-E, Sigma-Aldrich). Cell lines were maintained at 37°C in a humidified atmosphere of 95% air and 5% CO_2.

For immunocytochemistry, cells were fixed with 4% paraformaldehyde at 4°C for 10 min. After washing with 10 mM PBS three times, they were incubated for 1 h in a blocking solution (0.3% Triton-X, 2% goat serum, and 2% donkey serum in 0.1 M PBS) and then immunostained with a primary antibody against FLAG (1:1,000, Cat. No. F1804, Sigma-Aldrich) in a blocking solution at 4°C. After extensive washing, the cells on a cover glass were incubated with corresponding fluorescent secondary antibody Cy5 (1:500; Cat. No. 703-175-155, Jackson ImmunoResearch Laboratories) for 1.5 h at 24°C. Cells were washed with 10 mM PBS three times for 10 min and underwent additional incubation with DAPI (1:3,000, Cat. No. 62248, Pierce Biotech) for 7 min. Cells were again washed with 10 mM PBS twice for 10 min each time. Coverslips were mounted with fluorescent mounting medium (Cat. No. CS703, Dako) and dried. Then, a series of fluorescent images were obtained with a Nikon A1 confocal microscope.

2.5 | Polymerase chain reaction assay

Reverse transcriptase-quantitative polymerase chain reaction (RT-qPCR) was carried out using SYBR Green PCR Master Mix. In brief, reactions were performed in duplicates in a total volume of 10 mL containing 10 pM primer, 4 mL cDNA, and 5 mL power SYBR Green PCR Master Mix (Cat. No. 4367659, Applied Biosystems, Waltham, MA, USA). The mRNA level of radixin was normalized to that of glyceraldehyde 3-phosphate dehydrogenase (GAPDH) mRNA. Fold-induction was calculated using the 2–DDCT method.

RNA was isolated from HEK293 cells transfected with lentiviruses containing Rdx T564D or GFP using NucleoSpin Total RNA isolation kit (Cat. No. 740955.50, Macherey-Nagel, Dűren, Germany), and cDNA was generated by Maxime RT PreMix Oligo dT primer kit (Cat. No. 25081, Intron biotechnology, Seongnam-si, Korea). By performing RT-qPCR on the cDNA samples using ABI StepOne 2.1 Real-Time PCR System (Cat. No. 4376357, Applied Biosystems), the mRNA levels of radixin were measured. Primer sets for radixin purchased from Macrogen (Seoul, Korea) were as follows: radixin-qPCR-F (forward), GGTGTTGATGCTTTGGGTCT; radixin-qPCR-R (reverse), AGGTGCCTTTTTGTCGATTG. Thermal cycler conditions were as follows: 2 min at 50°C; 15 min at 95°C; followed by 40 cycles of 15 s at 95°C and 1 min at 60°C. GAPDH was used as an endogenous control to standardize the amount of RNA in each reaction.

2.6 | Surgery for virus injection

Rats were anesthetized with intraperitoneal (IP) ketamine (100 mg/kg) and xylazine (6 mg/kg), which are most widely and routinely used, and placed in a stereotaxic instrument with the incisor bar at 5.0 mm above the interaural line. Infusion cannulas (28 gauge; Plastics One) connected to 2 µl Hamilton syringes via PE-20 tubing were angled at 10° to the vertical and bilaterally lowered into the NAcc core (A/P, +3.2; L, ±2.8; D/V, –7.1 mm from bregma and skull). 1 µl (1×10^{12} particles/ml) of lentiviral constructs, containing copGFP alone or copGFP with Rdx T564D, were then bilaterally infused for 5 minutes and another 5 minutes allowed for diffusion before the infusion cannulas were raised. After viral infection was finished, the incised skin covering the skull was grabbed with surgical staplers. Then, rats were returned to their home cages for 2 weeks of recovery period, during which they were administered with an antibiotic, cefazolin (100 mg/kg, s.c.), and an anodynia, ketoprofen (5 mg/kg, s.c.), as needed to reduce animal pain.

2.7 | Design and procedure for animal experiment

We specified that this study was not pre-registered and exploratory. Upon arrival, all rats had a week-long adaptation period in the new housing environment, and four separate experiments were conducted.

Experiment 1 (western blotting of phosphorylated ERM by AMPH sensitization): Rats were arbitrarily divided into two groups, without specific randomization methods. Each rat was assigned based on cage number and permanent marker numbering on the tail. Rats in each group were pre-exposed to saline or AMPH (1.0 mg/kg, IP) with a total of four injections 2-3 days apart. This regimen of drug injection and the doses of the drugs used were previously shown to induce behavioral sensitization (Jang, Kim, Cho, Lee, & Kim, 2018; Kim, Perugini, Austin, & Vezina, 2001). Two weeks after the last pre-exposure injection, each group of rats was further arbitrarily divided into two subgroups, followed by a challenge injection with saline or AMPH (1.0 mg/kg, IP). After 60 min, they were decapitated, and their brain tissues (the NAcc core and shell) were prepared for western blot analysis. In this study, no exclusion criteria were predetermined. A total of 34 rats were used and all included in the statistical analysis.

Experiment 2 (western blotting of phosphorylated ERM by Rdx T564D): Rats were arbitrarily divided into two groups, in the same way as described in the Experiment 1, and they were surgically injected with viruses (GFP alone or GFP plus Rdx T564D, respectively). After two weeks at home cage, rats were decapitated, and their brain tissues (the NAcc core) were prepared for western blot analysis. In this study, no exclusion criteria were predetermined. A total of 20 rats were used and all included in the statistical analysis.

Experiment 3 (behavior and spine analyses with AMPH and Rdx T564D combined): Rats were arbitrarily divided into two groups, in the same way as described in the Experiment 1, and they were surgically injected with viruses (GFP alone or GFP plus Rdx T564D, respectively). Once they recovered from the surgery, each group of rats was further arbitrarily divided into two subgroups, without specific randomization methods, and pre-exposed to saline or AMPH (1.0 mg/kg, IP) with a total of four injections 2-3 days apart. This regimen of drug injection is known to produce enduring sensitization of the locomotor response to amphetamine (Jang et al., 2018; Kim et al., 2001). To avoid any confounding effects of conditioning, rats were administered AMPH in different places (i.e., in the activity boxes for the first and the fourth injections and in their home cages for the other injections). Two weeks after the last pre-exposure injection, all rats were first habituated to the activity boxes for 30 min and then injected with AMPH (1.0 mg/kg, IP), and their locomotor activity was measured for 1 h. The next day, the rats were transcardially perfused and their brains were removed. Using immunohistochemistry and confocal imaging, spine analyses were conducted by an experimenter who was aware of only the tissue numbers but was blinded to the group they belonged. In this study, no exclusion criteria were predetermined. A total of 23 rats were used and all included in the statistical analysis.

Experiment 4 (spine analysis with Rdx T564D alone): Rats were arbitrarily divided into two groups, in the same way as described in the Experiment 1, and they were surgically injected with viruses (GFP alone or GFP plus Rdx T564D, respectively). After two weeks at home cage, the rats were transcardially perfused and their brains were removed. Using immunohistochemistry and confocal imaging, spine analyses were conducted by an experimenter who was aware of only the tissue numbers but was blinded to the group they belonged. In this study, no exclusion criteria were predetermined. A total of 8 rats were used and all included in the statistical analysis.

2.8 | Locomotor activity

Locomotor activity was measured with a bank of 9 activity boxes (35 × 25 × 40 cm) (IWOO Scientific Corporation, Seoul, Korea) made of translucent Plexiglas. Each box was individually housed in a PVC plastic sound attenuating cubicle. The floor of each box consisted of 21 stainless steel rods (5 mm diameter) spaced 1.2 cm apart center-to-center. Two infrared light photobeams (Med Associates), positioned 4.5 cm above the floor and spaced evenly along the longitudinal axis of the box, were used to estimate horizontal locomotor activity.

2.9 | Tissue preparation and immunohistochemistry

Rats were all deeply anesthetized with ketamine (100 mg/kg) and xylazine (6 mg/kg) and then perfused transcardially with 10 mM phosphate buffered saline (PBS) (pH 7.4) followed by 4% paraformaldehyde solution (PFA) in 10 mM PBS (pH 7.4). The brains were removed and post-fixed overnight at 4°C in 4% PFA. Next day, the brains were washed with 10 mM PBS, cryoprotected in 30% sucrose solution and stored at −80°C.

Free-floating 100 μm sections from frozen tissue blocks were prepared on a cryostat (HM 525; Thermo Scientific). In order to enhance viral GFP signals, we adopted a method, which was previously shown to increase the brightness of sub-micron dendritic spines in infected neurons (Fakira, Massaly, Cohensedgh, Berman, & Moron, 2016; Wang et al., 2013). The tissue sections were blocked for 1 h in 10 mM PBS containing 5% normal goat serum (RRID: AB 2336990, Jackson ImmunoResearch Laboratories) and 0.3% triton X-100. Then, they were incubated overnight with the anti-TurboGFP antibody (1:1,000; Cat. No. AB501, Evrogen, Moscow, Russia), the anti-NeuN antibody (1:2,000; RRID: AB 10711040, Abcam), and the anti- glial fibrillary acidic protein (GFAP) antibody (1:1,000; Cat. No. 3670, Cell Signaling), diluted in 10 mM PBS containing 2% normal goat serum and 0.1% triton X-100 at 4°C. Next day, the sections were rinsed 3 times in 10 mM PBS containing 0.1% triton X-100 and incubated with the anti-rabbit IgG antibody coupled to Alexa 488 (1:2,000; RRID: AB 2576217, Invitrogen) or with the anti-mouse IgG antibody coupled to Alexa 568 (1:2,000; RRID: AB 2534072, Invitrogen) for 2 h at 24°C. They were rinsed again and cover-slipped with Vectashield mounting medium (Cat. No. H1400, Vector Laboratories).

2.10 | Imaging analysis for spines

For spine analysis, we imaged individual dendritic segments of medium spiny neurons (MSNs) following suggested requirements as in a previous publication (Cahill et al., 2018) [i.e., (i) the segments have

to show uniform GFP distribution, (ii) the segments cannot be overlapped with other neighboring dendritic segments and be traced back to their soma, (iii) secondary and tertiary dendritic segments at least 50μm from soma should be chosen]. The neurons that harbor minimum of three dendritic segments fulfilling such requirements were selected for spine analyses.

All images were acquired under a LSM700 confocal laser scanning microscope (Carl Zeiss) with a 488 nm argon laser. For whole cell reconstructions, confocal stacks of MSNs were imaged at 20x air objective lens (numerical aperture 0.7) with a Z-step size of 0.99 μm and an XY resolution of 0.417 μm. For dendrite imaging, dendritic segments stacks spaced 0.2 μm were acquired with a 63x oil-immersion objective (numerical aperture 1.4) and a scan zoom of 3.0. The pinhole aperture set to 1 Airy Unit and the line average of 2 was used. The full dynamic ranges of images were obtained by adjusting the laser intensity and photomultiplier tube gain. All images were taken with a resolution of 1024 pixels in X dimension. The Y dimension within the frame was cropped to ~ 300 pixels according to particular dendritic segments for fast image acquisition and the pixel dwell time was 1.58 μm/s. The final voxel size was $0.033 \times 0.033 \times 0.2\ \mu m^3$ in X-Y-Z plane.

To improve contrast and resolution, raw confocal images were deconvolved with AutoQuant X3 deconvolution software (Media Cybernetics, Inc.). Dendrite tracing and automatic spine detection was then performed using NeuronStudio software (RRID: SCR 013798; courtesy of Icahn School of Medicine at Mount Sinai, New York) with Rayburst algorithm (Rodriguez, Ehlenberger, Dickstein, Hof, & Wearne, 2008), which classifies spines into thin, mushroom or stubby according to the classification dimensions as follows: (i) Spines with head to neck diameter ratio greater than 1.1 are thin or mushroom, (ii) Spines that have a head diameter equal or greater than 0.35 μm are mushroom, (iii) Although spines do not meet head to neck diameter ratio greater than 1.1, they are categorized as thin if they have a spine length to head diameter ratio greater than 2.5, (iv) Spines that do not meet three conditions described above are stubby. The minimum and maximum values for spine height were set at 0.5 μm and 3.0 μm, respectively. For minimum stubby size, 22 voxels were set based on published criteria (Jung, Mulholland, Wiseman, Chandler, & Picciotto, 2013).

2.11 | Statistical analysis

Statistical analyses were performed using the Sigma Plot version 12.0 (Systat Software). The data were analyzed with either two-way analysis of variance (ANOVA), followed by Bonferroni post hoc test, or unpaired two-tailed Student's *t*-test. Shapiro-Wilk assessment for the normality test was carried out. The data on locomotor activity and spine densities were found to be normally distributed. The sample sizes of experiments were determined based on previous studies of a similar nature (Azocar et al., 2019; Xiong et al., 2018). No test for outlier were performed and no data were excluded. The cumulative frequency curves for dendritic spine head diameters and neck lengths were analyzed using Kolmogorov-Smirnov test. Possible correlations between locomotor activity and either spine density or thin spine length were examined using the Pearson correlation. Differences between experimental conditions were considered statistically significant when $p < 0.05$.

3 | RESULTS

3.1 | AMPH decreases ERM phosphorylation levels in the NAcc core, but not in the shell

We previously showed that phosphorylation levels of ERM proteins are significantly reduced by acute AMPH in the NAcc core (Kim et al., 2013). To further examine whether this is the case with AMPH sensitization, we measured phosphorylated ERM levels in the NAcc tissues (core and shell) (Figure 1a) obtained at 60 min after a challenge injection of AMPH (1 mg/kg) to rats pre-exposed to either saline or AMPH. Two-way ANOVA performed on the data obtained with the core showed multiple significant effects with pre-exposure ($F_{(1,30)} = 18.23$, $p < 0.001$), challenge ($F_{(1,30)} = 14.03$, $p < 0.001$), and pre-exposure × challenge interactions ($F_{(1,30)} = 5.01$, $p < 0.05$). Post hoc Bonferroni comparisons revealed that phosphorylation levels of ERM proteins were significantly reduced ($p < 0.05$–0.001) in rats with acute AMPH, consistent with our previous results (Kim et al., 2013), and in AMPH pre-exposed rats, regardless of challenge injections (Figure 1b). As shown previously (Kim et al., 2013), no significant differences were observed in the shell.

3.2 | Functional validation of Rdx T564D

To examine whether Rdx T564D is actually expressed when transfected inside the cell, we transduced it into HEK293 cells and confirmed its expression by detecting its tagging protein FLAG, along with GFP protein, especially near the cellular membranes (Figure S1). Then, we isolated total RNA from HEK293 cells transduced with either Rdx T564D or GFP alone. With amplification of radixin mRNA by RT-qPCR, we confirmed that Rdx T564D was overexpressed in the cell (Figure S2).

Next, to examine whether Rdx T564D functions to the change of phosphorylation levels of ERM in the NAcc core, we measured phosphorylated and total ERM levels in the NAcc core obtained after two weeks of virus infection. Interestingly, the expression of Rdx T564D in the NAcc core significantly reduced the phosphorylation levels of ERM proteins ($t_{18} = 3.92$, $p < 0.001$) in this site, whereas it had no effect on the total levels of ERM proteins (Figure S3).

3.3 | Rdx T564D is expressed on neuronal cells, but not on glial cells, in the NAcc core

To examine on which cell type in the nucleus accumbens (NAcc) core Rdx T564D is expressed, we observed co-labelling of GFP with either NeuN or GFAP, specific biomarkers for neuronal and glial cells,

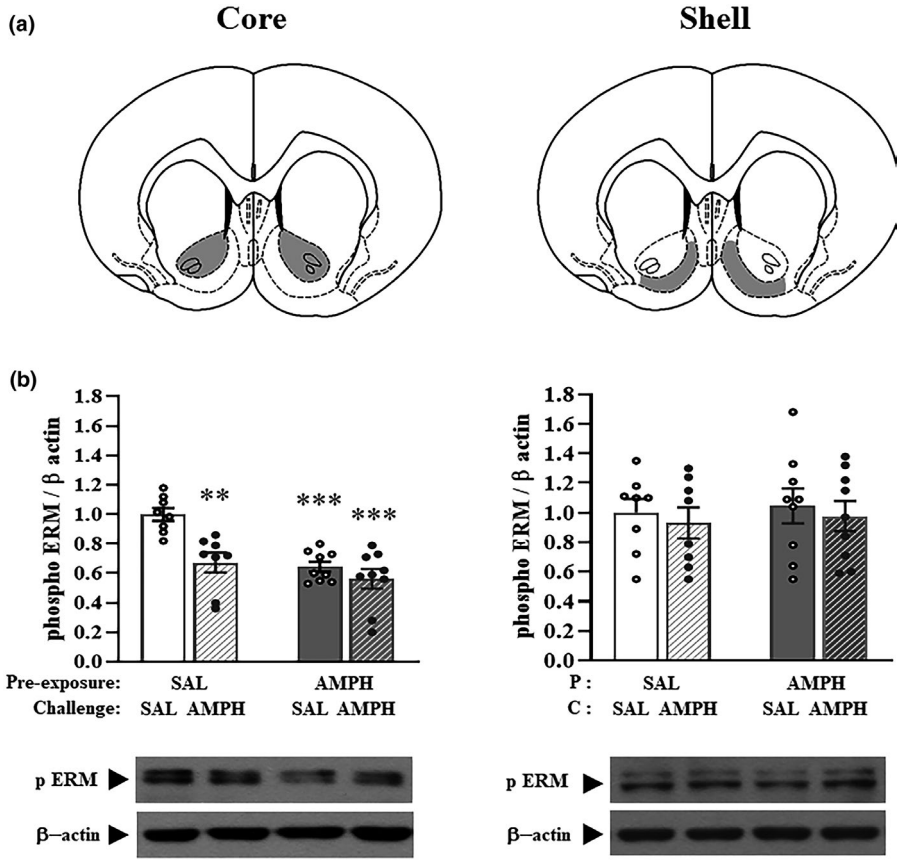

FIGURE 1 The phosphorylation levels of ezrin-radixin-moesin (ERM) proteins were decreased in the nucleus accumbens (NAcc) core, but not in the shell, by acute and chronic amphetamine (AMPH). (a) The NAcc core and shell region where tissues were taken out is shown (dark grey areas). Tissues were prepared bilaterally and pooled for each individual animal's protein isolation. Line drawing is from Paxinos and Watson (2004) and depicts the caudal surface of a coronal section extending 1.70–2.70 mm from bregma. (b) Quantification of the levels of phosphorylated ERM protein and the representative Western blots are shown. Values for the band intensities were first normalized to β-actin in each group and expressed as mean + standard error of mean relative to saline pre-exposure + saline challenge control group. $^{**}p<0.01$, $^{***}p<0.001$, compared to saline pre-exposure + saline challenge control group. Numbers of rats analyzed for each group are as follows: Saline pre-exposure + Saline challenge (8 rats), Saline pre-exposure + AMPH challenge (8), AMPH pre-exposure + Saline challenge (9), AMPH pre-exposure + AMPH challenge (9)

after two weeks of virus injection. Fluorescent microscopy images reveal that NeuN was co-localized with GFP (white arrows overlapped, Figure 2a), whereas GFAP was localized separately from GFP (white and yellow arrows not overlapped, Figure 2b).

3.4 | Rdx T564D in the NAcc core inhibits the development of AMPH-induced locomotor sensitization

The experimental scheme, from virus injection surgery to behavioral sensitization, is depicted in Figure 3a. The target area, the NAcc core into which viruses were microinjected, is indicated in a schematic drawing of the brain, and a couple of representative pictures (low and high magnification, respectively) showing the MSNs emitting green fluorescence are also shown (Figure 3b). After 2 weeks of virus expression, rats were placed for behavioral sensitization schedule with AMPH, and challenged with it following another 2 weeks of drug-free withdrawal period. Two-way ANOVA conducted on the 1-h total locomotor activity counts showed significant effects of pre-exposure ($F_{(1,19)} = 13.96$, $p < 0.01$) and pre-exposure × virus interactions ($F_{(1,19)} = 6.71$, $p < 0.05$). Post hoc Bonferroni comparisons revealed that locomotor activity was significantly increased ($p < 0.001$) in AMPH pre-exposed rats compared to saline pre-exposed rats with GFP control virus, whereas significant increase of locomotor activity was absent in AMPH pre-exposed rats with Rdx T564D virus (Figure 3c). Time-course analyses of these findings showed that the ability of Rdx T564D to inhibit the AMPH-induced locomotor sensitization observed in AMPH pre-exposed rats with GFP control virus was apparent throughout the 1-h time course (Figure 3d).

3.5 | Rdx T564D induces quantitative changes of dendritic spines in the NAcc core

Representative dendritic segments from different groups and an enlarged portion, indicating different subtypes of spines and

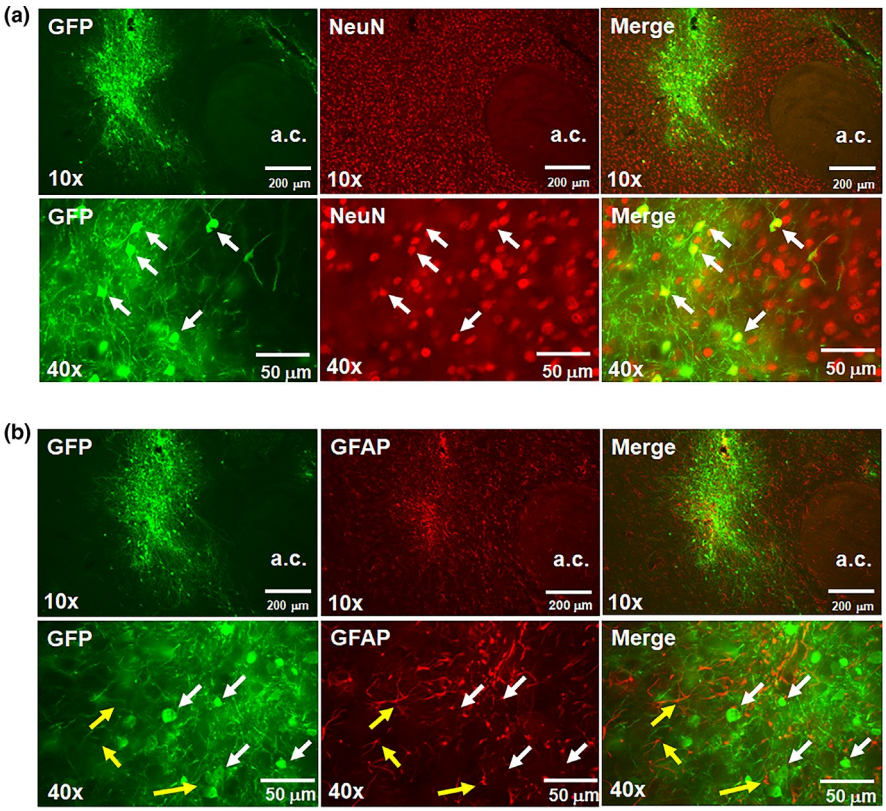

FIGURE 2 A phosphomimetic pseudo-active mutant of radixin (Rdx T564D) was expressed on neuronal cells, but not on glial cells, in the nucleus accumbens (NAcc) core. (a) Representative fluorescent microscopy images showing co-localization (indicated by white arrows) of green fluorescent protein (GFP) and NeuN, a specific biomarker for neurons, in the NAcc core after two weeks of virus injection. Green and red indicates GFP and NeuN expression, respectively, while yellow indicates co-localization of the two proteins. The scale bars are 200 and 50 μm for 10X and 40X magnifications, respectively. (b) Representative fluorescent microscopy images showing the expressions of green fluorescent protein (GFP) and glial fibrillary acidic protein (GFAP), a specific biomarker for glial cells, in the NAcc core after two weeks of virus injection. Green and red indicates GFP and GFAP expression, respectively. No co-localization was found between two proteins (white arrows indicating GFP and yellow arrows indicating GFAP are not overlapped). The scale bars are 200 and 50 μm for 10X and 40X magnifications, respectively. a.c.: anterior commissure

measurements of head diameter and spine length, are shown in Figures 4a, b. The total spine densities were counted in several randomly selected MSNs (16 to 22 neurons per group) in the NAcc core and found to be increased in rats with Rdx T564D, similar to rats showing AMPH sensitization (Figure 4c). Two-way ANOVA conducted on the total spine density showed a significant effect of pre-exposure × virus interactions ($F_{(1,70)} = 7.78$, $p < 0.01$). Post hoc Bonferroni comparisons revealed that total spine density was significantly increased ($p < 0.05$) in saline pre-exposed rats with Rdx T564D virus compared to saline pre-exposed rats with GFP control virus, whereas it did not reach statistical significance in AMPH pre-exposed rats with Rdx T564D virus (Figure 4c). AMPH sensitization alone with GFP control virus reached statistical significance compared to acute AMPH with GFP control ($p < 0.01$). Interestingly, the thin spine densities, but not mushroom and stubby spine densities, were also found to be increased in rats with Rdx T564D, AMPH sensitization, and both (Figure 4d, S4a, b). Two-way ANOVA conducted on the thin spine density showed a significant effect of pre-exposure × virus interactions ($F_{(1,70)} = 6.45$, $p < 0.05$). Post hoc Bonferroni comparisons revealed that thin spine density was significantly increased ($p < 0.05$–0.01) in all other groups compared to saline pre-exposed rats with GFP control virus (Figure 4d). These results indicate that the density changes that appeared in MSNs in the NAcc core induced by Rdx T564D or AMPH sensitization are mostly caused by thin spines.

3.6 | Rdx T564D increases thin spine length in the NAcc core

We measured head diameters and spine lengths for all individual spines in each group and compared them between the groups. Thus, qualitative differences in the spines were revealed. We found that Rdx T564D significantly promoted the increase of thin spine lengths, but did not affect head diameters, in the AMPH acute and sensitization groups (Figure 5a, b). Cumulative frequency plots of spine length for thin spines revealed significant rightward shifts when Rdx T564D was present ($p < 0.05$–0.01, Kolmogorov–Smirnov test). Interestingly, these effects were not observed after AMPH sensitization alone. For mushroom spines, Rdx T564D significantly

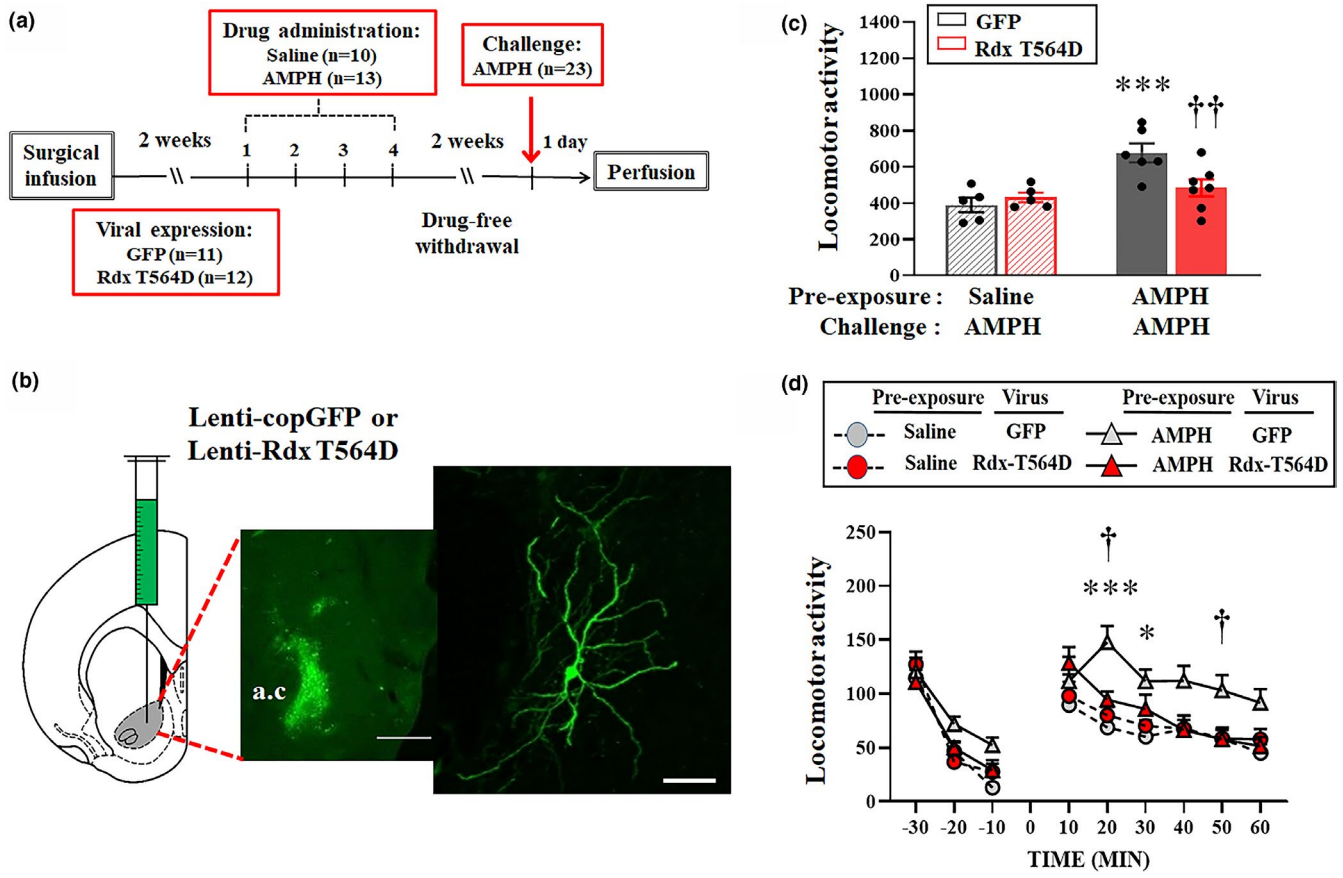

FIGURE 3 A phosphomimetic pseudo-active mutant of radixin (Rdx T564D) in the nucleus accumbens (NAcc) core inhibits the expression of amphetamine (AMPH)-induced locomotor sensitization. (a) Time lines for the experimental procedures indicate the duration of virus expression and the locomotor sensitization scheme. (b) The NAcc core region where viruses were injected is schematically illustrated (dark grey area). A representative low magnification (2x) epifluorescence image of the NAcc core expressing lentivirus-mediated copepod green fluorescent protein (copGFP) and a higher magnification (20x) confocal microscopy image of a single neuron in this region are also shown. Scale bars are 1 mm and 50 μm, respectively. (c) Total locomotor activity counts observed during the 60 min test on AMPH challenge are shown as group mean + standard error of mean (SEM). $^{***}p < 0.001$, compared between saline and AMPH pre-exposures within GFP. $^{\dagger\dagger}p < 0.01$, compared between GFP and Rdx T564D within AMPH pre-exposures. Numbers of rats analyzed for each group are as follows: Saline pre-exposure + AMPH challenge with GFP (5 rats), Saline pre-exposure + AMPH challenge with Rdx T564D (5), AMPH pre-exposure + AMPH challenge with GFP (6), AMPH pre-exposure + AMPH challenge with Rdx T564D (7). (d) Time-course data are shown as group mean (+ SEM) locomotor activity counts with 10 min intervals obtained during the 30 min preceding (−30 through 0 min) and the 60 min following AMPH challenge (0–60 min). $^{*}p < 0.05$, $^{***}p < 0.001$, compared between saline and AMPH pre-exposures within GFP. $^{\dagger}p < 0.05$, compared between GFP and Rdx T564D within AMPH pre-exposures

increased spine lengths with acute AMPH, but this effect disappeared with AMPH sensitization (Figure S5a, b). No changes were observed in stubby spines (Figure S6a, b). To further examine details of the spine lengths, we divided the lengths at 0.5 μm intervals, from 0.5 (minimum) to 3.0 (maximum) μm. Two-way ANOVA conducted on the spine length intervals for thin spines showed significant effects of interval ($F_{(4,150)} = 59.23$, $p < 0.001$) and virus × interval interactions ($F_{(4,150)} = 5.43$, $p < 0.001$). Post hoc Bonferroni comparisons revealed that there were significant decreases in the percentage of thin spines for the interval between 1.0 and 1.5 μm ($p < 0.01$–0.001) in the presence of Rdx T564D in AMPH acute and sensitization groups, while there was an additional significant increase for the interval between 1.5 and 2.0 μm ($p < 0.01$) (Figure 5c). These effects were not observed with mushroom and stubby spines (Figure S5c, S6c).

3.7 | Rdx T564D inhibits the development of AMPH sensitization by selectively increasing filopodia-like thin spines in the NAcc core

Considering that Rdx T564D, as a phosphomimetic pseudo-active mutant, supposedly drives thin spines to immaturity (Furutani et al., 2007; Yoshihara et al., 2009), our present findings that it increased overall thin spine lengths suggest that there might be an actual increase in filopodia-like (i.e., immature) thin spines. To examine this possibility, we looked at the density distributions of all individual spines with kernel density estimates spread in two dimensions: head diameters and spine lengths per group. Next, we drew lines at 0.2 μm of head diameter (almost the middle) and 1.5 μm of spine length (based on Figure 5c) to divide the whole distributions into four arbitrary areas, numbering areas 1 to 4 (Figure 6a). Interestingly, we

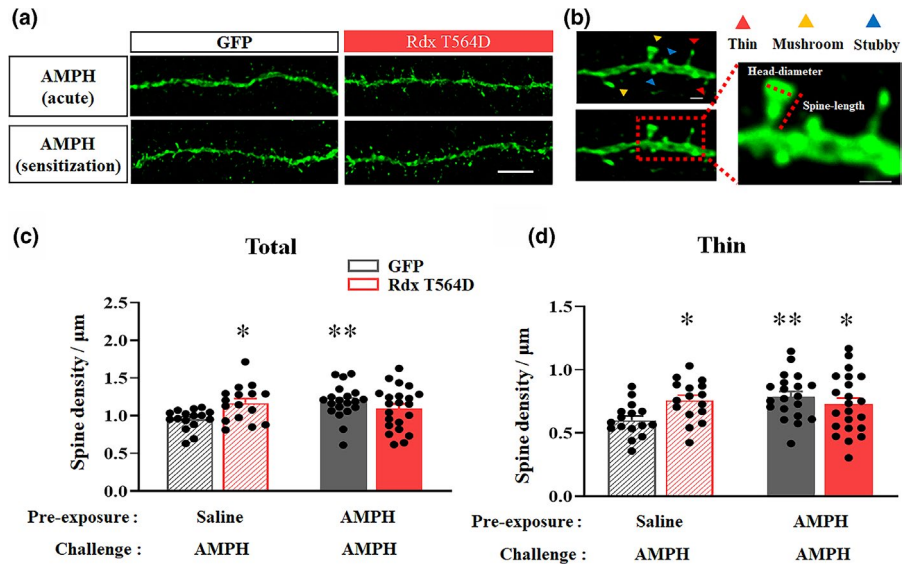

FIGURE 4 Effects of a phosphomimetic pseudo-active mutant of radixin (Rdx T564D) and amphetamine (AMPH) sensitization on spine densities in the nucleus accumbens (NAcc) core. (a) Representative high resolution images of a dendritic segment labelled with green fluorescent protein (GFP) from each group. Images were obtained at magnification of 63x and with additional magnification of zoom 2.5 from ZEN software. Scale bar is 5 μm. (b) A representative image of a GFP-labeled dendritic segment showing spine subtypes. Dotted lines enlarged a portion of dendritic segment and qualitatively delineate spine morphology (i.e., head-diameter and spine-length). Scale bar is 1 μm. (c) Significant differences of densities were observed for total (left) and thin (right) spines in the NAcc core between groups. $^{*}p < 0.05$, $^{**}p < 0.01$, compared to saline pre-exposure with GFP control group. Data are shown as mean + standard error of mean. Numbers of neurons analyzed for each group are as follows: Saline-GFP (16 neurons from 5 rats), Saline-Rdx T564D (16, 5), AMPH-GFP (20, 6), AMPH-Rdx T564D (22, 7)

found that there was an evident trend that Rdx T564D pulled density distributions toward area 4 (thinner and longer) with a concomitant density dilution in area 1 (thicker and shorter) in acute AMPH and AMPH sensitization as well. In contrast, AMPH sensitization by itself maintained the density distribution patterns similar to acute AMPH. Based upon these findings, we distinguished thin spines into two types, filopodia-like (immature), with head diameter less than 0.2 μm and spine length greater than 1.5 μm (in area 4), and mature for the rest (in areas 1–3). Next, we re-measured the densities of each type of thin spine. Two-way ANOVA performed on these data showed significant effects of pre-exposure × virus interactions ($F_{(1,70)} = 5.39$, $p < 0.05$) for mature thin spines, and virus ($F_{(1,70)} = 8.62$, $p < 0.01$) for filopodia-like thin spines. Post hoc Bonferroni comparisons revealed that mature thin spines were significantly increased ($p < 0.01$) only in AMPH sensitization, whereas filopodia-like thin spines were significantly increased ($p < 0.05$) only with Rdx T564D (Figure 6b).

3.8 | Correlation analysis between locomotor activity and dendritic spines

To examine whether dendritic spines have correlation with locomotor activity, we conducted correlation analyses on data obtained from rats with different virus (GFP vs. Rdx T564D) and AMPH (acute vs. sensitization) conditions. It was found that there was no significant correlation between spine densities and locomotor activity in any groups (Figure S7). However, there was a significant negative correlation revealed between thin spine length (filopodia-like) and locomotor activity in AMPH sensitization with GFP group ($r = 0.83$, $p < 0.05$) (Figure S8).

3.9 | Rdx T564D by itself increases filopodia-like thin spines in the NAcc core

To examine whether Rdx T564D contributes to the change of spines in the NAcc core, either by itself or by the influence of AMPH, we further analyzed spine densities in MSNs obtained from rats with viruses but no AMPH exposed. The total and thin spine densities were found to be increased in rats with Rdx T564D compared to GFP control ($t_{28} = 2.29$, $p < 0.05$; $t_{28} = 3.26$, $p < 0.01$, respectively) (Figure 7a). The mushroom and stubby spine densities were not observed to be significant (Figure S9). Further analysis of thin spines into two types, filopodia-like (immature), with head diameter less than 0.2 μm and spine length greater than 1.5 μm, and mature for the rest, revealed that filopodia-like, but not mature, thin spine densities were increased in rats with Rdx T564D compared to GFP control ($t_{28} = 4.23$, $p < 0.001$) (Figure 7b).

4 | DISCUSSION

We demonstrated that the phosphorylation levels of ERM in the NAcc core were decreased with the regimen of AMPH injection to

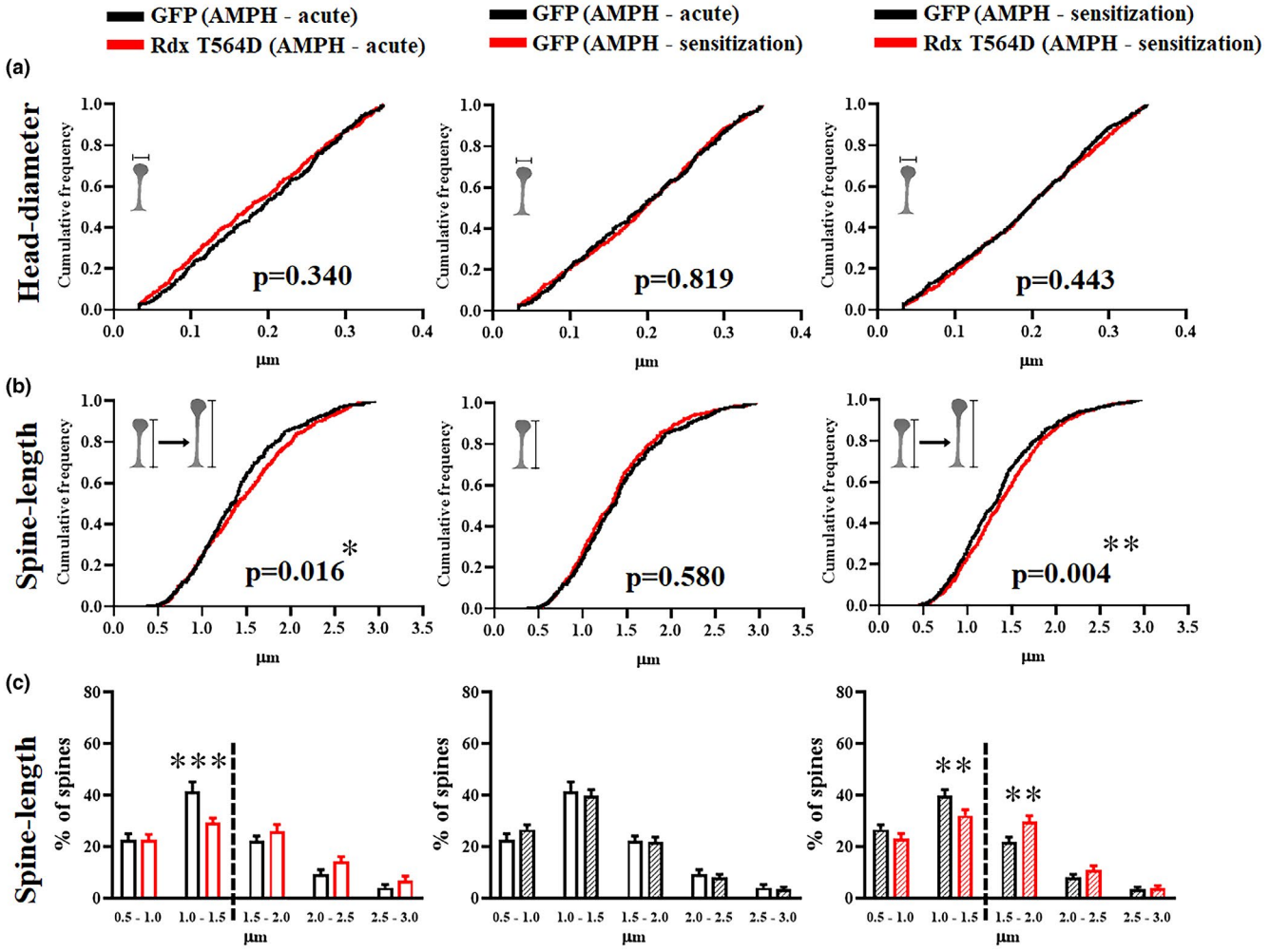

FIGURE 5 Cumulative frequency plots of head-diameter and spine-length for thin spine. (a) Cumulative frequency plots of head-diameter for whole thin spines show no significant changes between groups. (b) Cumulative frequency plots of spine-length for whole thin spines revealed significant rightward shifts when a phosphomimetic pseudo-active mutant of radixin (Rdx T564D) was present in both amphetamine (AMPH) acute (*left*) and sensitization (*right*) groups (*$p < 0.05$, **$p < 0.01$ by Kolmogorov–Smirnov test). AMPH sensitization alone produced no significant differences from AMPH acute (*middle*). Numbers of thin spines and neurons analyzed for each group's cumulative frequency are as follows: AMPH acute with green fluorescent protein (GFP) (401 spines in 16 neurons), AMPH acute with Rdx T564D (538, 16), AMPH sensitization with GFP (684, 20), AMPH sensitization with Rdx T564D (779, 22). (c) Histograms (0.5 μm intervals from 0.5 to 3.0 μm) of spine-length for thin spines per neuron revealed significant changes in specific intervals in the presence of Rdx T564D compared to GFP in AMPH acute (decrease in 1.0–1.5 μm interval, *left*) or sensitization (decrease in 1.0–1.5 μm and increase in 1.5–2.0 μm intervals, *right*) groups. **$p < 0.01$, ***$p < 0.001$, comparison between GFP and Rdx T564D. Data are shown as mean + standard error of mean. Numbers of neurons analyzed for each group are as follows: Saline-GFP (16 neurons from 5 rats), Saline-Rdx T564D (16, 5), AMPH-GFP (20, 6), AMPH-Rdx T564D (22, 7)

induce behavioral sensitization (Figure 1b). These results suggest that phosphorylation levels of ERM might be important regulator for the expression of AMPH sensitization. Actually, with the same regimen, we showed that AMPH produced no behavioral sensitization with the expression of Rdx T564D in the NAcc core (Figure 3c). As Rdx T564D, an artificially designed radixin mutant by replacing threonine with aspartic acid at amino acid 564 residue, acts as a phosphomimetic pseudo-active mutant (Furutani et al., 2007; Riecken et al., 2016), its inhibitory effects on AMPH sensitization is considered to be caused by the increase of pseudo-phosphorylated (active) status of radixin. On the contrary, Rdx T564D by itself contributes to reduce phosphorylation levels of ERM in the NAcc core (Figure S3), which might look contradictory to explain the role of phosphorylation levels of ERM. However, transfection of Rdx T564D overwhelmingly expressed mutant radixin mRNA in the cell as shown by RT-qPCR (Figure S2), which will be functionally enough (active) to overcome reduction (inactive) of phosphorylation levels of ERM in the NAcc core. Although it is a somewhat mystery how phosphorylation levels of ERM were reduced after Rdx T564D transfection, it could be possible that endogenous phosphorylation form of ERM might be reduced in response to the presence of huge amount of pseudo-active mutant by compensation mechanism. It remains to be explored in the future.

Consistent with previous findings (Li et al., 2004; Robinson & Kolb, 2004), we observed that AMPH sensitization, compared to

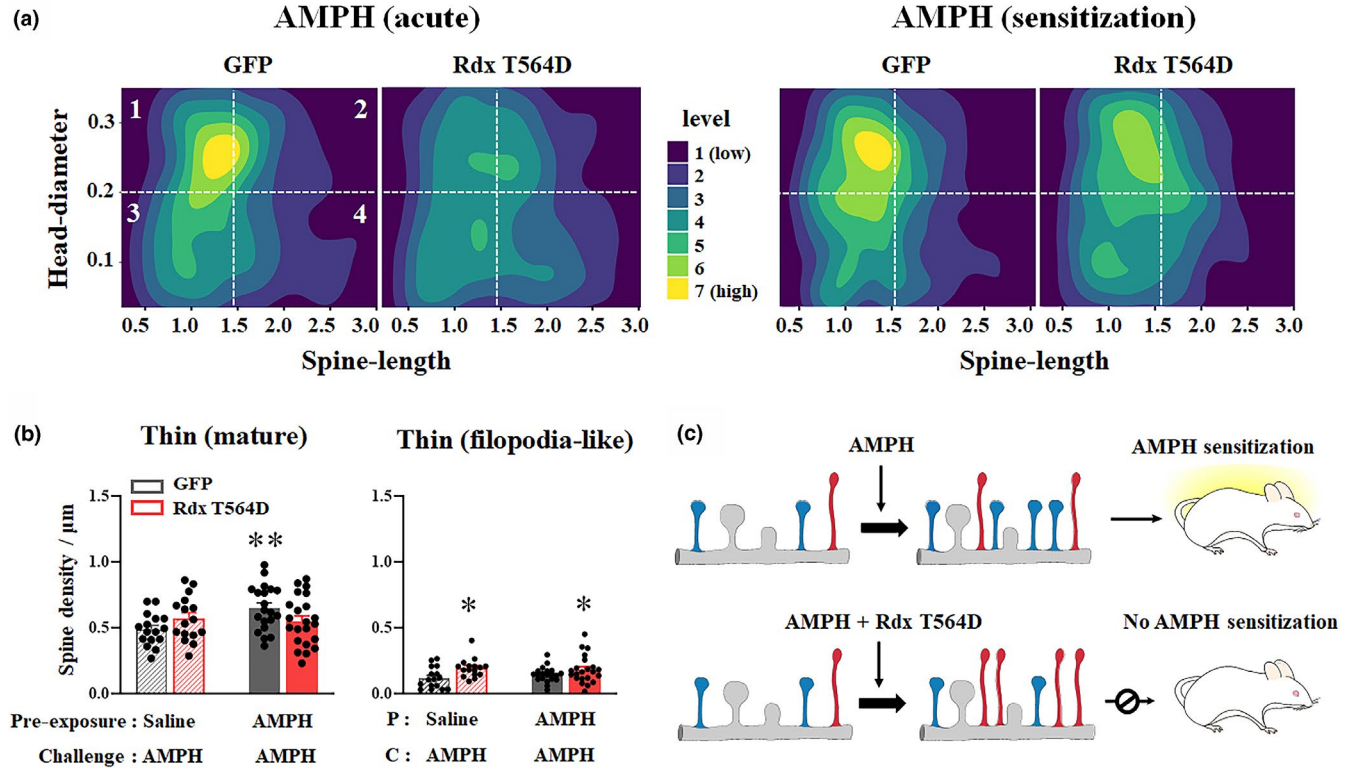

FIGURE 6 A phosphomimetic pseudo-active mutant of radixin (Rdx T564D) inhibits the expression of amphetamine (AMPH) sensitization by selectively increasing filopodia-like thin spines in the nucleus accumbens (NAcc) core. (a) 2D density contour plots with kernel density estimates show the density distributions of thin spines according to their head-diameters (Y-axis) and spine-lengths (X-axis). Dotted lines are drawn at 0.2 μm of head-diameter and 1.5 μm of spine-length to divide whole distributions into 4 arbitrary areas numbered with 1–4. Relative density levels are indicated by colors from violet (low) to yellow (high). It is evident that Rdx T564D pulled density distributions of thin spines away from area 1 (thick head-diameter and short spine-length) toward area 4 (thin head-diameter and long spine-length) both in AMPH acute and sensitization. (b) Thin spines were separated and re-counted according to sizes of head-diameters and spine-lengths. As a result, thin spines with lower than 0.2 μm of head-diameters and higher than 1.5 μm of spine-lengths (equivalent to area 4) were grouped as filopodia-like thin spines, while all the rest were grouped as mature thin spines (equivalent to areas 1–3). For mature thin spines, significant difference of density was observed only in AMPH sensitization group compared to AMPH acute group, in the presence of green fluorescent protein (GFP) (*left*). For filopodia-like thin spines, significant difference of densities was observed only when Rdx T564D was present in both AMPH acute and AMPH sensitization groups (*right*). $^{*}p < 0.05$, $^{**}p < 0.01$, compared to AMPH acute with GFP group. Data are shown as mean + standard error of mean (SEM). Numbers of neurons analyzed for each group are as follows: Saline-GFP (16 neurons from 5 rats), Saline-Rdx T564D (16, 5), AMPH-GFP (20, 6), AMPH-Rdx T564D (22, 7). (c) AMPH sensitization and its inhibition according to the state of dendritic spines in the NAcc core are illustrated. Chronic AMPH upon its challenge produces the increase of the densities of both mature and filopodia-like thin spines, with no changes of their ratio compared to acute AMPH, and subsequent expression of AMPH sensitization. However, in the presence of Rdx T564D in the NAcc core, it produces relatively higher density of filopodia-like thin spines, resulting in the inhibition of the expression of AMPH sensitization

AMPH acute in the absence of Rdx T564D, increased the spine density in the NAcc core (Figure 4c), and further revealed that it was specifically thin spines among the subtypes (Figure 4d). Considering that thin spines are generally thought to be more flexible and undergo structural changes in response to diverse neuronal stimuli (Bourne & Harris, 2007; Chidambaram et al., 2019; Trachtenberg et al., 2002), our present results may reflect the adaptation process of MSNs in this site toward repeated injections of AMPH. In contrast to thin spines, the densities of mushroom and stubby spines were not observed significantly changed in AMPH sensitized rats (Figure S4), which is not surprising as mushroom and stubby spines are generally thought to be more stable (Bourne & Harris, 2007; Chidambaram et al., 2019; Trachtenberg et al., 2002). Interestingly, a study reported that AMPH sensitization increased the phosphorylation levels of AMPA receptors, but not their expression levels, at the cell surface of NAcc MSNs (Wang et al., 2017). Considering that the numbers of synaptic AMPA receptors are well correlated with the spine head size (Kasai, Matsuzaki, Noguchi, Yasumatsu, & Nakahara, 2003; Matsuzaki et al., 2001), these results may imply that there might be no increase of spine densities with big head size (e.g., mushroom and stubby spines). Our present findings show that AMPH sensitization actually induced no significant changes in the densities of mushroom and stubby spines reflecting biochemical findings at this site.

Similar to AMPH sensitization, Rdx T564D also produced an increase in spine density, either with AMPH acute (total) or with

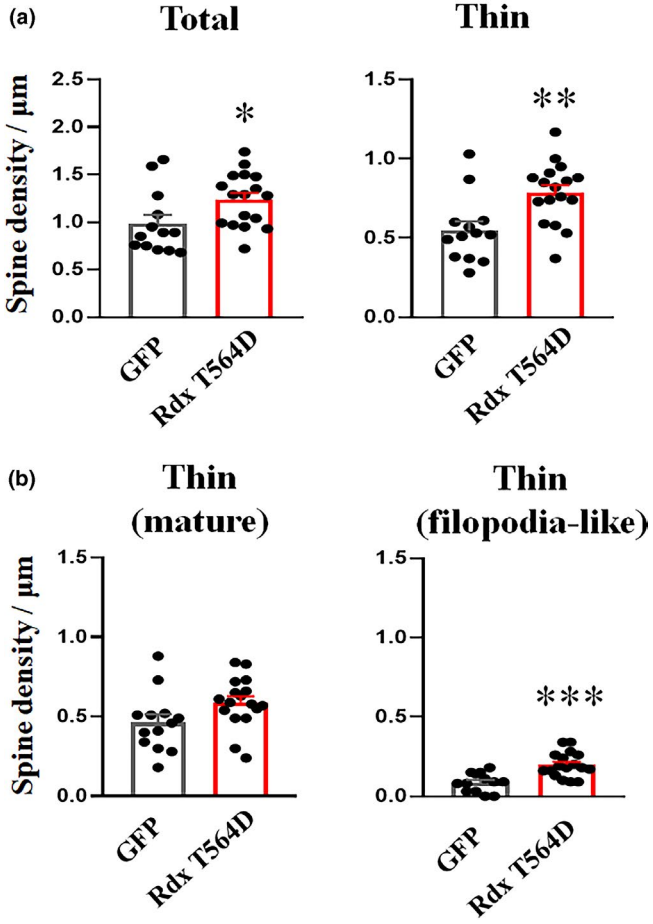

FIGURE 7 Effects of a phosphomimetic pseudo-active mutant of radixin (Rdx T564D) on spine densities in the nucleus accumbens (NAcc) core. (a) Significant differences of densities were observed for total and thin spines in the NAcc core between groups. (b) Thin spines were separated and re-counted according to sizes of head-diameters and spine-lengths. As a result, thin spines with lower than 0.2 μm of head-diameters and higher than 1.5 μm of spine-lengths were grouped as filopodia-like thin spines, while all the rest were grouped as mature thin spines. Significant difference of densities was observed for filopodia-like thin spines, whereas it was not observed for mature thin spines. $^{*}p < 0.05$, $^{**}p < 0.01$, $^{***}p < 0.001$, compared to green fluorescent protein (GFP) control group. Data are shown as mean + standard error of mean. Numbers of neurons analyzed for each group are as follows: GFP (13 neurons from 4 rats) and Rdx T564D (17, 4)

AMPH sensitization (total and thin) (Figure 4c, d). Moreover, Rdx T564D alone with no AMPH exposed produced an increase in spine density (total and thin) (Figure 7a). These results indicate that Rdx T564D by itself has the ability to increase spine density regardless of AMPH. However, considering that ERM proteins negatively regulate spine maturity by binding to cell adhesion molecules like ICAM-5 when phosphorylation levels are increased at the C-terminal region (Furutani et al., 2007, 2012; Raemaekers et al., 2012; Yoshihara et al., 2009), our present finding that the quantitative increment of spine density with Rdx T564D, which mimics the increase of radixin phosphorylation, seems superficially contradictory. To resolve this conflict, we further examined the qualitative differences in spine changes between the groups. It turns out that AMPH sensitization by itself produced no changes in thin spine lengths compared to AMPH acute (*middle*, Figure 5b). However, Rdx T564D promoted their lengths in conditions with AMPH (acute and sensitization) (*left and right*, Figure 5b). Reflecting this finding, when we separated thin spines by its length into two subtypes, mature and filopodia-like, we found that the density of filopodia-like thin spines was significantly increased, whereas that of mature thin spines was not, in conditions with AMPH (acute and sensitization) (Figure 6b), or even without it as well (Figure 7b).

When we further analyzed thin spine lengths with respect to the 0.5 μm intervals, Rdx T564D contributed the most to the reduction of the percentage of thin spines with spine length between 1.0 and 1.5 μm (Figure 5c). In contrast, the percentages of thin spines with lengths more than 1.5 μm were slightly increased throughout the lengths up to 3.0 μm, except for the interval between 1.5 and 2.0 μm where there was statistical significance with AMPH sensitization. These results suggest that there is a trend for the overall percentage of thin spines with their lengths, from a decrease to increase at 1.5 μm as a branch point. The 2D contour plots of thin spine density distributions according to their head-diameters and spine-lengths evidently reveal that Rdx T564D pulled density distributions of thin spines away from the status with thick head-diameter and short spine-length toward the status with thin head-diameter and long spine-length both in AMPH acute and sensitization (Figure 6a). It is known that the speed of excitatory postsynaptic currents is influenced by morphological changes of dendritic spines (Cathala, Holderith, Nusser, DiGregorio, & Cull-Candy, 2005; Holtmaat & Svoboda, 2009; Michaluk et al., 2011). Furthermore, it has also been shown that excitatory postsynaptic potential amplitudes are negatively correlated with spine neck lengths (Araya, Jiang, Eisenthal, & Yuste, 2006; Araya, Vogels, & Yuste, 2014). Thus, it is difficult for long-necked spines to generate significant somatic cell depolarization. Taking these into account, our present findings suggest that the synaptic strengths mediated by thin spines of MSNs in the NAcc core in the presence of Rdx T564D may be relatively weak because of the increase in spine lengths. Therefore, it may disrupt synaptic signaling that the normal development of AMPH sensitization requires, which will eventually contribute to the inhibition of its expression (see Figures 3c, 5b, and 6a).

In the line of comparing dendritic spines with behavioral sensitization, we attempted correlation analyses between two parameters. Although there was no significant correlation between spine density and locomotor activity in all groups (Figure S7), we found that the length of filopodia-like thin spines is negatively correlated with locomotor activity solely in AMPH sensitization with GFP group (Figure S8). These results suggest that the length of filopodia-like thin spines may be an important contributing factor negatively regulating the expression of locomotor sensitization, which is consistent with our present findings that actual length of thin spines was increased (Figure 5b), resulting in the increase of density of filopodia-like thin spines (Figure 6b), in AMPH sensitization group with Rdx T564D,

and thereby the expression of locomotor sensitization was inhibited in this group (Figure 3c). However, as we had a very few number of rats to get a significant correlation, a caution should be taken to apply this data for whole interpretation.

Collectively, the present results indicate that although Rdx T564D contributes to the increase of thin spine densities similar to AMPH sensitization (Figure 4d), their qualities are different in that the former is more likely to increase filopodia-like long thin spines, whereas the latter does more mature thin spines (Figure 6b). As clearly shown in the 2D density contour plot (Figure 6a), Rdx T564D disturbs the density distribution pattern of thin spines with AMPH sensitization, which may affect the adaptation process during the development of AMPH sensitization that normally requires mature thin spines (Figure 6c). These results will eventually lead to the inhibition of the development of AMPH sensitization (Figure 3c and 6c).

Considering our limited knowledge about concrete functional roles of dendritic spines, it will be inappropriate to causally link the quantitative and even qualitative changes of spines to the differential expression of a certain type of behavior, including addiction (Russo et al., 2010). Furthermore, it has been reported that the changes in dendritic spines in the NAcc could be separated from behavioral changes in addiction in some conditions (Anderson et al., 2017; Pulipparacharuvil et al., 2008; Singer et al., 2009). Nonetheless, it is also certain that dendritic spines are important in making associative contributions to long-term behavioral changes (Brown et al., 2011; Robinson & Kolb, 2004; Wang et al., 2013; Xu et al., 2009; Yang et al., 2009). As development of addiction requires a complex process with multiple stages, dynamic alteration of spine changes may contribute to the ongoing process either early or later (Christian et al., 2017), and thereby eventually affect the expression of addictive behaviors.

Although ERM proteins are known to play important regulatory roles in spine formation and maturation as well as cellular signaling in neuronal cells, their function in the brain, especially in relation to addiction, is not well understood. Very recently, it has been shown that ezrin knockdown in the NAcc core reduced astroglial synaptic associations and potentiated cued heroin seeking (Kruyer, Scofield, Wood, Reissner, & Kalivas, 2019). Furthermore, radixin and moesin have been previously shown to play a significant role in other types of learning and memory (Freymuth & Fitzsimons, 2017; Hausrat et al., 2015). In this regard, considering that AMPH sensitization is a form of long-term memory induced by drugs of abuse and their interaction with environments (Anagnostaras et al., 2002; Robinson & Berridge, 1993), our present findings that manipulation of functionally active radixin levels in the NAcc core can lead to the disruption of AMPH sensitization, by affecting the quality and density distribution of thin spines at this site, will obviously add a piece of new evidence about the important functional role of ERM proteins in the brain.

ACKNOWLEDGEMENTS

This work was supported by the National Research Foundation of Korea funded by the Ministry of Science and ICT (2018R1A4A1025230, 2019R1A2C1011262, 2019R1A2C2089518). All experiments were in compliance with the ARRIVE guidelines.

CONFLICT OF INTEREST

The authors declare that they have no conflict of interest.

AUTHOR CONTRIBUTIONS

W.T.C., W.Y.K. and J.-H.K. designed the experiments; W.T.C. and W.Y.K. performed the western blotting experiments; W.T.C. and H.R. performed the animal and imaging experiments; W.T.C., W.Y.K., M.J.K. and J.-H.K. performed dendritic analyses; S.E.L. prepared virus particles, performed cell transfection experiment and PCR assay; L.R. and H.M. designed and provided plasmids for viral vectors; W.T.C., W.Y.K. and J.-H.K. wrote the paper; W.T.C., W.Y.K., M.J.K., S.E.L. and J.-H.K. prepared the figures. All authors read and approved the final manuscript.

DATA AVAILABILITY STATEMENT

Data available on request from the authors.

ORCID

Jeong-Hoon Kim https://orcid.org/0000-0001-7095-3729

REFERENCES

Anagnostaras, S. G., Schallert, T., & Robinson, T. E. (2002). Memory processes governing amphetamine-induced psychomotor sensitization. *Neuropsychopharmacology*, 26, 703–715.

Anderson, E. M., Wissman, A. M., Chemplanikal, J., Buzin, N., Guzman, D., Larson, E. B., Neve, R. L., Nestler, E. J., Cowan, C. W., & Self, D. W. (2017). BDNF-TrkB controls cocaine-induced dendritic spines in rodent nucleus accumbens dissociated from increases in addictive behaviors. *Proceedings of the National Academy of Sciences of the United States of America*, 114, 9469–9474.

Araya, R., Jiang, J., Eisenthal, K. B., & Yuste, R. (2006). The spine neck filters membrane potentials. *Proceedings of the National Academy of Sciences of the United States of America*, 103, 17961–17966.

Araya, R., Vogels, T. P., & Yuste, R. (2014). Activity-dependent dendritic spine neck changes are correlated with synaptic strength. *Proceedings of the National Academy of Sciences of the United States of America*, 111, E2895–E2904.

Azocar, V. H., Sepúlveda, G., Ruiz, C., Aguilera, C., Andres, M. E., & Fuentealba, J. A. (2019). The blocking of kappa-opioid receptor reverses the changes in dorsolateral striatum dopamine dynamics during the amphetamine sensitization. *Journal of Neurochemistry*, 148, 348–358.

Bourne, J., & Harris, K. M. (2007). Do thin spines learn to be mushroom spines that remember? *Current Opinion in Neurobiology*, 17, 381–386.

Bretscher, A., Edwards, K., & Fehon, R. G. (2002). ERM proteins and merlin: integrators at the cell cortex. *Nature Review Molecular Cell Biology*, 3, 586–599.

Brown, T. E., Lee, B. R., Mu, P., Ferguson, D., Dietz, D., Ohnishi, Y. N., Lin, Y., Suska, A., Ishikawa, M., Huang, Y. H., Shen, H., Kalivas, P. W., Sorg, B. A., Zukin, R. S., Nestler, E. J., Dong, Y., & Schlüter, O. M. (2011). A silent synapse-based mechanism for cocaine-induced locomotor sensitization. *Journal of Neuroscience*, 31, 8163–8174.

Cahill, M. E., Walker, D. M., Gancarz, A. M., Wang, Z. J., Lardner, C. K., Bagot, R. C., Neve, R. L., Dietz, D. M., & Nestler, E. J. (2018).

The dendritic spine morphogenic effects of repeated cocaine use occur through the regulation of serum response factor signaling. *Molecular Psychiatry*, 23, 1474–1486.

Cathala, L., Holderith, N. B., Nusser, Z., DiGregorio, D. A., & Cull-Candy, S. G. (2005). Changes in synaptic structure underlie the developmental speeding of AMPA receptor-mediated EPSCs. *Nature Neuroscience*, 8, 1310–1318.

Chidambaram, S. B., Rathipriya, A. G., Bolla, S. R., Bhat, A., Ray, B., Mahalakshmi, A. M., Manivasagam, T., Thenmozhi, A. J., Essa, M. M., Guillemin, G. J., Chandra, R., & Sakharkar, M. K. (2019). Dendritic spines: Revisiting the physiological role. *Progress in Neuropsyhcopharmacology & Biological Psychiatry*, 92, 161–193.

Christian, D. T., Wang, X., Chen, E. L., Sehgal, L. K., Ghassemlou, M. N., Miao, J. J., Estepanian, D., Araghi, C. H., Stutzmann, G. E., & Wolf, M. E. (2017). Dynamic alterations of rat nucleus accumbens dendritic spines over 2 months of abstinence from extended-access cocaine self-administration. *Neuropsychopharmacology*, 42, 748–756.

Fakira, A. K., Massaly, N., Cohensedgh, O., Berman, A., & Moron, J. A. (2016). Morphine-associated contextual cues induce structural plasticity in hippocampal CA1 pyramidal neurons. *Neuropsychopharmacology*, 41, 2668–2678.

Freymuth, P. S., & Fitzsimons, H. L. (2017). The ERM protein moesin is essential for neuronal morphogenesis and long-term memory in Drosophila. *Molecular Brain*, 10, 41.

Furutani, Y., Kawasaki, M., Matsuno, H., Mitsui, S., Mori, K., & Yoshihara, Y. (2007). Interaction between telencephalin and ERM family proteins mediates dendritic filopodia formation. *Journal of Neuroscience*, 27, 8866–8876.

Furutani, Y., Kawasaki, M., Matsuno, H., Mitsui, S., Mori, K., & Yoshihara, Y. (2012). Vitronectin induces phosphoryaltion of ezrin/radixin/moesin actin-binding proteins through binding to its novel neuronal receptor telencephalin. *Journal of Biological Chemistry*, 287, 39041–39049.

Hausrat, T. J., Muhia, M., Gerrow, K., Thomas, P., Hirdes, W., Tsukita, S., Heisler, F., Herich, L., Dubroqua, S., Breiden, P., Feldon, J., Schwarz, J. R., Yee, B. K., Smart, T. G., Triller, A., & Kneussel, M. (2015). Radixin regulates synaptic GABAA receptor density and is essential for reversal learning and short-term memory. *Nature Communications*, 6, 6872.

Holtmaat, A., & Svoboda, K. (2009). Experience-dependent structural synaptic plasticity in the mammalian brain. *Nature Review Neuroscience*, 10, 647–658.

Jang, J. K., Kim, W. Y., Cho, B. R., Lee, J. W., & Kim, J. H. (2018). Locomotor sensitization is expressed by ghrelin and D1 dopamine receptor agonist in the nucleus accumbens core in amphetamine pre-exposed rat. *Addiction Biology*, 23, 849–856.

Jung, Y., Mulholland, P. J., Wiseman, S. L., Chandler, L. J., & Picciotto, M. R. (2013). Constitutive knockout of the membrane cytoskeleton protein beta adducin decreases mushroom spine density in the nucleus accumbens but does not prevent spine remodeling in response to cocaine. *European Journal of Neuroscience*, 37, 1–9.

Kasai, H., Matsuzaki, M., Noguchi, J., Yasumatsu, N., & Nakahara, H. (2003). Structure-stability-function relationships of dendritic spines. *Trends in Neuroscience*, 26, 360–368.

Kim, J. H., Perugini, M., Austin, J. D., & Vezina, P. (2001). Previous exposure to amphetamine enhances the subsequent locomotor response to a D1 dopamine receptor agonist when glutamate reuptake is inhibited. *Journal of Neuroscience*, 21, RC133.

Kim, W. Y., Jang, J. K., Shin, J. K., & Kim, J. H. (2013). Amphetamine dephosphorylates ERM proteins in the nucleus accumbens core and lithium attenuates its effects. *Neuroscience Letters*, 552, 103–107.

Kruyer, A., Scofield, M. D., Wood, D., Reissner, K. J., & Kalivas, P. W. (2019). Heroin cue-evoked astrocytic structural palsticity at nucleus accumbens synapses inhbits heroin seeking. *Biological Psychiatry*, 86, 811–819.

Li, Y., Acerbo, M. J., & Robinson, T. E. (2004). The induction of behavioural sensitization is associated with cocaine-induced structural plasticity in the core (but not shell) of the nucleus accumbens. *European Journal of Neuroscience*, 20, 1647–1654.

Louvet-Vallée, S. (2000). ERM proteins: from cellular architecture to cell signaling. *Biology of the Cell*, 92, 305–316.

Matsuzaki, M., Ellis-Davies, G. C., Nemoto, T., Miyashita, Y., Iino, M., & Kasai, H. (2001). Dendritic spine geometry is critical for AMPA receptor expression in hippocampal CA1 pyramidal neurons. *Nature Neuroscience*, 4, 1086–1092.

Matus, A. (2005). Growth of dendritic spines: a continuing story. *Current Opinion in Neurobiology*, 15, 67–72.

Michaluk, P., Wawrzyniak, M., Alot, P., Szczot, M., Wyrembek, P., Mercik, K., Medvedev, N., Wilczek, E., De Roo, M., Zuschratter, W., Muller, D., Wilczynski, G. M., Mozrzymas, J. W., Stewart, M. G., Kaczmarek, L., & Wlodarczyk, J. (2011). Influence of matrix metalloproteinase MMP-9 on dendritic spine morphology. *Journal of Cell Science*, 124, 3369–3380.

Neisch, A. L., & Fehon, R. G. (2011). Ezrin, radixin and moesin: key regulators of membrane-cortex interactions and signaling. *Current Opinion in Cell Biology*, 23, 377–382.

Niggli, V., & Rossy, J. (2008). Ezrin/radixin/moesin: Versatile controllers of signaling molecules and of the cortical cytoskeleton. *International Journal of Biochemistry & Cell Biology*, 40, 344–349.

Paxinos, G., & Watson, C. (2004). *The rat brain in stereotaxic coordinates* (Fourth ed.). Elsevier Academic Press.

Pulipparacharuvil, S., Renthal, W., Hale, C. F., Taniguchi, M., Xiao, G., Kumar, A., Russo, S. J., Sikder, D., Dewey, C. M., Davis, M. M., Greengard, P., Nairn, A. C., Nestler, E. J., & Cowan, C. W. (2008). Cocaine regulates MEF2 to control synaptic and behavioral plasticity. *Neuron*, 59, 621–633.

Raemaekers, T., Peric, A., Baatsen, P., Sannerud, R., Declerck, I., Baert, V., Michiels, C., & Annaert, W. (2012). ARF6-mediated endosomal transport of telencephalin affects dendritic filopodia-to-spine maturation. *The EMBO Journal*, 31, 3252–3269.

Riecken, L. B., Zoch, A., Wiehl, U., Reichert, S., Scholl, I., Cui, Y., Ziemer, M., Anderegg, U., Hagel, C., & Morrison, H. (2016). CPI-17 drives oncogenic Ras signaling in human melanomas via Ezrin-Radixin-Moesin family proteins. *Oncotarget*, 7, 78242–78254.

Robinson, T. E., & Berridge, K. C. (1993). The neural basis of drug craving: an incentive- sensitization theory of addiction. *Brain Research Reviews*, 18, 247–291.

Robinson, T. E., & Kolb, B. (1997). Persistent structural modifications in nucleus accumbens and prefrontal cortex neurons produced by previous experience with amphetamine. *Journal of Neuroscience*, 17, 8491–8497.

Robinson, T. E., & Kolb, B. (1999). Alterations in the morphology of dendrites and dendritic spines in the nucleus accumbens and prefrontal cortex following repeated treatment with amphetamine or cocaine. *European Journal of Neuroscience*, 11, 1598–1604.

Robinson, T. E., & Kolb, B. (2004). Structural plasticity associated with exposure to drugs of abuse. *Neuropharmacology*, 47(Suppl 1), 33–46.

Rodriguez, A., Ehlenberger, D. B., Dickstein, D. L., Hof, P. R., & Wearne, S. (2008). Automated three-dimensional detection and shape classification of dendritic spines from fluorescence microscopy images. *PLoS One*, 3, e1997.

Russo, S. J., Dietz, D. M., Dumitriu, D., Morrison, J. H., Malenka, R. C., & Nestler, E. J. (2010). The addicted synapse: mechanisms of synaptic and structural plasticity in nucleus accumbens. *Trends in Neuroscience*, 33, 267–276.

Singer, B. F., Tanabe, L. M., Gorny, G., Jake-Matthews, C., Li, Y., Kolb, B., & Vezina, P. (2009). Amphetamine-induced changes in dendritic morphology in rat forebrain correspond to associative drug conditioning rather than nonassociative drug sensitization. *Biological Psychiatry*, 65, 835–840.

Trachtenberg, J. T., Chen, B. E., Knott, G. W., Feng, G., Sanes, J. R., Welker, E., & Svoboda, K. (2002). Long-term in vivo imaging of experience-dependent synaptic plasticity in adult cortex. *Nature*, 420, 788–794.

Vezina, P. (2004). Sensitization of midbrain dopamine neuron reactivity and the self-administration of psychomotor stimulant drugs. *Neuroscience and Biobehavioral Reviews*, 27, 827–839.

Wang, X., Cahill, M. E., Werner, C. T., Christoffel, D. J., Golden, S. A., Xie, Z., Loweth, J. A., Marinelli, M., Russo, S. J., Penzes, P., & Wolf, M. E. (2013). Kalirin-7 mediates cocaine-induced AMPA receptor and spine plasticity, enabling incentive sensitization. *Journal of Neuroscience*, 33, 11012–11022.

Wang, Q., Li, D., Bubula, N., Campioni, M. R., McGehee, D. S., & Vezina, P. (2017). Sensitizing exposure to amphetamine increases AMPA receptor phosphorylation without increasing cell surface expression in the rat nucleus accumbens. *Neuropharmacology*, 117, 328–337.

Xiong, L., Meng, Q., Sun, X., Lu, X., Fu, Q., Peng, Q., Yang, J., Oh, K. W., & Hu, Z. (2018). Cociane- and amphetamne-regulated transcript peptide in the nucleus accumbens shell inhibits cocaine-induced locomotor sensitization to transient ober-expression of α-$Ca^{2+/}$calmodulin-dependent protein kinase II. *Journal of Neurochemistry*, 146, 289–303.

Xu, T., Yu, X., Perlik, A. J., Tobin, W. F., Zweig, J. A., Tennant, K., Jones, T., & Zuo, Y. (2009). Rapid formation and selective stabilization of synapses for enduring motor memories. *Nature*, 462, 915–919.

Yang, G., Pan, F., & Gan, W. B. (2009). Stably maintained dendritic spines are associated with lifelong memories. *Nature*, 462, 920–924.

Yoshihara, Y., De Roo, M., & Muller, D. (2009). Dendritic spine formation and stabilization. *Current Opinion in Neurobiology*, 19, 146–153.

SUPPORTING INFORMATION

Additional supporting information may be found in the online version of the article at the publisher's website.

How to cite this article: Cai, WT, Kim, WY, Kwak, MJ, Rim, H, Lee, SE, Riecken, LB et al. (2022) Disruption of amphetamine sensitization by alteration of dendritic thin spines in the nucleus accumbens core. *Journal of Neurochemistry*. 00:1–15. https://doi.org/10.1111/jnc.15582